Temporal dynamics of GABA and Glx in the visual cortex

Reuben Rideaux*
Department of Psychology, Downing Street, University of Cambridge, CB2 3EB, UK
*reuben.rideaux@gmail.com

ABSTRACT

Magnetic resonance spectroscopy (MRS) can be used in vivo to differentiate types of neural activity, e.g., inhibitory and excitatory, and provide evidence for the involvement of different neurotransmitter systems in cognitive processes. The relatively low signal-to-noise of MRS measurements has shaped the types of questions that it has been used to address. In particular, temporal resolution is often sacrificed in MRS studies to achieve sufficient signal to produce a reliable estimate of metabolite concentration. Here we apply novel analyses with large datasets to reveal the dynamics of GABA+ and Glx in the visual cortex, and compare this with changes in the posterior cingulate cortex. We find that the dynamic concentrations of GABA+ and Glx in the visual cortex drifts in opposite directions, that is, GABA+ decreased while Glx increases over time. Further, we find that in both the visual and posterior cingulate cortices, the concentration of GABA+ predicts that of Glx ~30 sec later, such that an increase in GABA+ is correlated with a subsequent reduction in Glx. Together, these results expose novel temporal trends and interdependencies of primary neurotransmitters both locally, in the visual cortex, and globally, across multiple brain regions. More broadly, we demonstrate the feasibility of using MRS to investigate in vivo dynamic changes of metabolites.

Keywords: Magnetic resonance spectroscopy; visual cortex; GABA; Glx; temporal dynamics

INTRODUCTION

Magnetic resonance spectroscopy (MRS) can be used in vivo to measure the concentration of metabolites within the brain. Whereas the blood-oxygen-level-dependent signal measured using functional magnetic resonance imaging (fMRI) cannot distinguish between different systems of activity, e.g., excitatory and inhibitory, measuring the concentration of neurotransmitters within the brain with MRS can begin to differentiate between these systems. For the purpose of understanding neural mechanisms, identifying the involvement of neurotransmitter systems that support cognitive processes can be more informative than locating regions of neural representation.

A common approach used to identify metabolite involvement in cognitive processes with MRS is to measure the concentration of metabolites in a group of participants, within a brain region of interest, and test whether individual variance of a particular metabolite is related to performance on a task supported by the cognitive process. For example, concentration of the inhibitory neurotransmitter γ-aminobutyric acid (GABA) in the visual cortex is positively related with visual discrimination of orientation (Edden, Muthukumaraswamy, Freeman, & Singh, 2009; Kurcyus et al., 2018; Mikkelsen, Harris, Edden, & Puts, 2018). This evidence has been interpreted as indicating that sharp neuronal tuning for orientation is supported by inhibition. Another, less common, approach used to identify metabolite involvement is to measure baseline metabolite concentration while a participant is “at rest” and compare this with another measurement taken while the participant performs a task. A difference metabolite concentration observed between the two measurements may be taken as evidence of its involvement in the cognitive processes supporting the task. For example, GABA concentration in the visual cortex is different when participants view stereoscopic images comprised of both light and dark features, compared to just light or dark features (Rideaux, Goncalves, & Welchman, 2019). This has been interpreted as evidence for the increased involvement of inhibition in visual processing of combined light and dark features.

While MRS can be used to differentiate types of activity within the brain, compared to fMRI it is severely limited in terms of its temporal resolution, which is constrained by the signal-to-noise ratio of measurements acquired using the technique. Although the duration that restricts the temporal resolution of MRS (i.e., the relaxation time) can be similar to that of fMRI (i.e., ~2s), in order to yield a reliable measurement of metabolite concentration from within the brain, multiple samples must be combined to reach a sufficient signal-to-noise ratio. For example, it is common to combine between 200-300 acquisitions (~10 min) to produce a single measure of metabolite concentration. This approach, while often necessary, obscures observation of changes in metabolite concentration that occur during this period.

Here we overcome the signal-to-noise limitation of MRS by applying temporal analyses of metabolite concentration to a large dataset of participants. We measure the dynamic concentration of GABA and Glx in the visual cortex of human participants while at rest, from a dataset containing 69 scans. We compare these results with data from the posterior cingulate cortex of 196 participants at rest (Mikkelsen et al., 2017, 2019). To observe the dynamics of metabolites, we process the data in two ways. We first take a moving average of a ~6 min period, which reveals low frequency trends in the data. Next, using a new technique, we combine data across participants (rather than time), which allows us to track the concentration of metabolites with relatively high temporal resolution (6 sec) over a 13 min period. This novel approach exposes large changes in GABA+ and Glx, previously obscured by averaging over long durations. Further, we reveal a striking relationship between GABA+ and Glx, which is present in both datasets (i.e., visual and posterior cingulate cortices): a change in GABA+ predicts the opposite change in Glx ~30 sec later.

The relative low signal-to-noise of MRS has shaped the approaches with which the technique has been used to study the brain. Here we overcome this limitation by using a new technique that combines measurements across a large sample of data, which reveals novel dynamic trends and interactions within and between neurotransmitters.

METHODS

Participants

Fifty-eight healthy participants from the University of Cambridge with normal or corrected-to-normal vision participated in the experiment. The mean age was 24.4 yr (range = 19.4–40.5 yr; 31 women). Nine of the participants, including the author (RR), repeated the experiment twice and one participant repeated three times, on different days; thus, the total number of scans was sixty-nine. Participants were screened for contra-indications to MRI prior to the experiment. All experiments were conducted in accordance with the ethical guidelines of the Declaration of Helsinki and were approved by the University of Cambridge STEM and all participants provided informed consent.

Data collection

Participants underwent a MR spectroscopic acquisition targeting the visual cortex at the Cognition and Brain Sciences Unit (Cambridge, UK). During the acquisition, the lights in the room were turned off and participants were instructed to close their eyes. To compare these with data measured from another brain region, we reanalysed previously gathered MR spectroscopic data targeting the posterior cingulate cortex (Mikkelsen et al., 2017, 2019). For the purpose of further comparison, we also reanalysed data from a study investigating metabolite concentrations in the visual cortex under different viewing conditions (Kurcyus et al., 2018).

Data acquisition

Magnetic resonance scanning targeting visual cortex was conducted on a 3T Siemens Prisma equipped with a 32-channel head coil. Anatomical T1-weighted images were acquired for spectroscopic voxel placement with an ‘MP-RAGE’ sequence. For detection of GABA+ (GABA and co-edited macromolecules) and Glx (a complex comprising Glutamate and Glutamine), spectra were acquired using a MEGA-PRESS sequence: TE=68ms, TR=3000ms; 256 transients of 2048 data points were acquired in 13 min experiment time; a 14.28 ms Gaussian editing pulse was applied at 1.9 (ON) and 7.5 (OFF) ppm; water unsuppressed 16 transients. Water suppression was achieved using variable power with optimized relaxation delays (VAPOR) and outer volume suppression (OVS). Automated shimming followed by manual shimming was conducted to achieve approximately 12 Hz water linewidth.

The following data from the “Big GABA” dataset was used in the current study: G4, G5, G7, G8, P1, P3, P4, P5, P6, P7, P8, P10, S1, S6, & S8. We used the macromolecule unsuppressed acquisitions from these datasets for closer comparison with the visual cortex data, and we excluded data from G1 and G6 as these had fewer acquisitions. A detailed description of the data acquisitions for these datasets can be found in (Mikkelsen et al., 2017,

2019). To summarize the procedure, magnetic resonance scanning targeting posterior cingulate cortex was conducted on 3T Siemens, GE, and Phillips scanners equipped with 8-, 32-, or 64- channel head coils. Spectra were acquired using a MEGA-PRESS sequence: TE=68ms, TR=2000ms; 320 transients of either 2048 or 4096 data points were acquired in 12 min experiment time; a 15 ms Gaussian editing pulse was applied at 1.9 (ON) and 7.5 (OFF) ppm.

Spectra were acquired from a location targeting visual cortex, i.e., V1/V2 (**Fig. 1a**), and posterior cingulate cortex (**Fig. 1b**). The voxel targeting the visual cortex (3×3×2 cm) was placed medially in the occipital lobe; the lower face aligned with the cerebellar tentorium and positioned so to avoid including the sagittal sinus and to ensure it remained within the occipital lobe. The voxel targeting the posterior cingulate cortex (3×3×3 cm) was positioned in the medial parietal lobe and rotated in the sagittal plane to align with a line connecting the genu and splenium of the corpus callosum. The DICOM of the voxel location was used as a mask to calculate the volume of grey matter (GM), white matter (WM), and cerebral spinal fluid (CSF) within each voxel. The proportion of grey matter (GM), white matter (WM), and cerebral spinal fluid (CSF) in each voxel was used to apply a CSF-correction (Kreis, Ernst, & Ross, 1993) to the metabolite measurements with the following equation:

$$C_{tisscorr} = \frac{C_{meas}}{f_{GM} + f_{WM}} \quad (1)$$

where $C_{tisscorr}$ and C_{meas} are the CSF-corrected and uncorrected metabolite concentrations, respectively, and f_{GM} and f_{WM} are the proportion of GM and WM within the voxel. Segmentation was performed using the Statistical Parametric Mapping toolbox for MATLAB (SPM12, http://www.fil.ion.ucl.ac.uk/spm/).

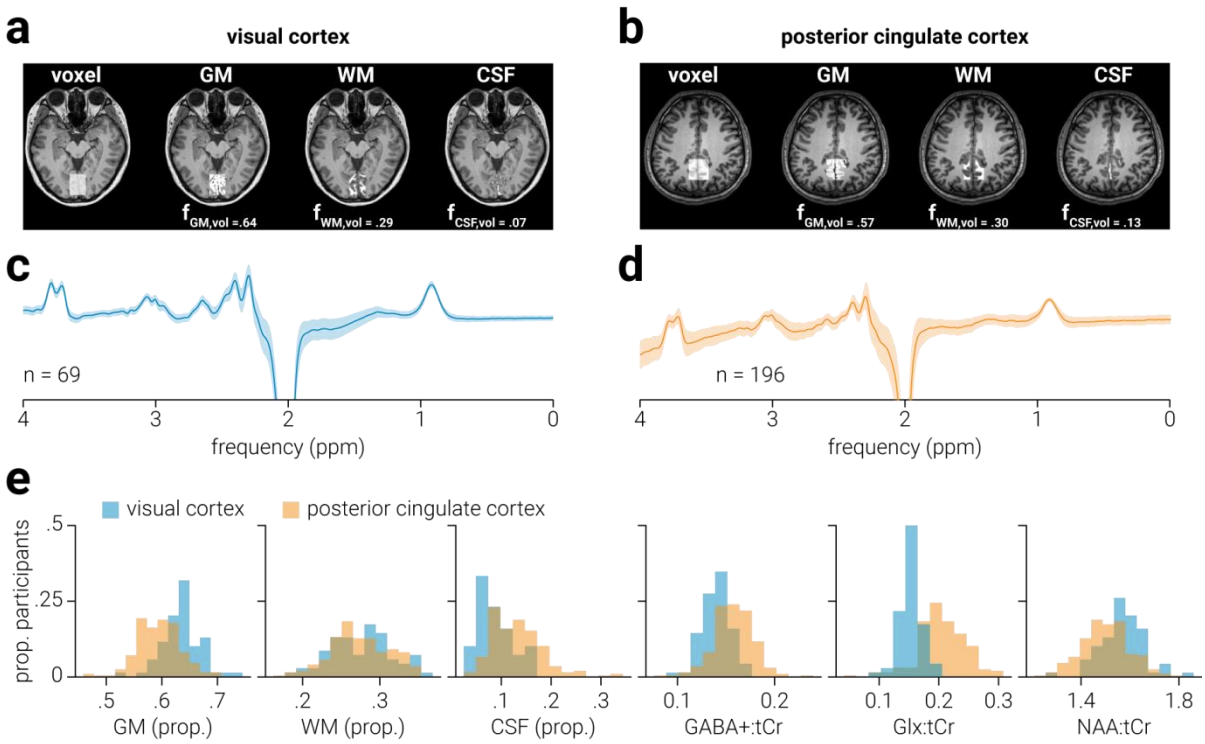

Figure 1. Data acquisition. Representative MRS voxel placement for **a**) visual and **b**) posterior cingulate cortices on a T1-weighted structural image and probabilistic partial volume voxel maps following tissue segmentation for one participant. Corresponding tissue proportions of grey matter (GM), white matter (WM) and cerebrospinal fluid (CSF) are shown. Average spectra across all subjects for **c**) visual and **d**) posterior cingulate cortices; number of subjects comprising each average spectrum is shown and grey shaded regions indicate standard deviation. **e**) Distribution of (GM, WM, CSF) voxel tissue proportions, and (GABA+, Glx, NAA) metabolite concentrations across participants for visual and posterior cingulate cortices.

In addition to the abovementioned primary datasets, we also reanalysed a subset of the data from (Kurcyus et al., 2018); scans for which the authors had access to in individual acquisition format (as opposed to a scan average). The dataset we reanalysed comprised 29, 27, and 28 measurements from an MRS voxel targeting V1, while participants had their eyes closed, open in darkness, or open while viewing an alternating checkerboard stimulus, respectively. A detailed description of the data acquisitions is provided in (Kurcyus et al., 2018). To summarize the procedure, magnetic resonance scanning targeting visual cortex was conducted on a 3T Siemens Biograph mMR system equipped a 12-channel head coil. Spectra were acquired using a MEGA-PRESS sequence: TE=68ms, TR=2000ms; 256 transients of 2048 data points were acquired in 8.6 min experiment time; editing J-refocusing pulse irradiated at 1.9 (ON) and 7.5 (OFF) ppm.

Data processing

Spectral quantification was conducted in MATLAB using GANNET v3.1 (Edden, Puts, Harris, Barker, & Evans, 2014; www.gannetmrs.com) and in-house scripts. Individual spectra were frequency and phase corrected to the Choline and Creatine peaks. Total creatine (tCr)

signal intensity was determined by fitting a single Lorentzian peak to the mean non-edited spectra. N-acetylaspartate (NAA) signal intensity was determined by fitting a single Lorentzian peak to the mean 'OFF' spectra. 'ON' and 'OFF' spectra were subtracted to produce the edited spectrum (**Fig. 1c** & **d**), from which GABA+ and Glx signal intensity were modelled off single- and double- Gaussian peaks, respectively. Intensities of GABA+, Glx, and NAA were normalized to the commonly used internal reference tCr (Jansen, Backes, Nicolay, & Kooi, 2006), yielding relative concentration values (i.e., GABA+:tCr, Glx:tCr, and NAA:tCr; **Fig. 1e**). The tCr signal is acquired within the same MEGA-PRESS acquisitions as the target metabolites; thus, normalization of GABA+, Glx, and NAA to tCr minimizes the influence of subject movement during the scan and eliminates the effects of chemical shift displacement (Mullins et al., 2014). Further, if changes occur during the acquisition which alter the entire spectrum (e.g., changes in signal strength, line width, or dilution associated with changes in blood flow (Ip et al., 2017)) this will produce no change in the ratio of target metabolites to tCr.

Table 1 shows the average full width at half maximum (FWHM) and frequency drift of the "static" spectra, i.e., spectra averaged across all acquisitions, across subjects for measurements taken from the visual cortex (VC) and posterior cingulate cortex (PCC) from the primary datasets. The fitting error for GABA+, Glx, NAA, and tCr were divided by the amplitude of their fitted peaks to produce normalized measures of uncertainty. The average fit error for each metabolite was relatively low (**Table 1**; Mullins et al., 2014; Rowland et al., 2016). One outlier was omitted from the posterior cingulate cortex dataset prior to calculation of the summary statistics shown in Table 1.

Table 1. Measures of spectral quality and fit error

Location	FWHM				Frequency	Fit error			
	GABA+	Glx	NAA	tCr	drift (std. Hz)	GABA+	Glx	NAA	tCr
VC	21.6±1.2	17.8±0.4	8.7±1.4	8.7±1.5	1.1±0.5	10.1±2.2	1.3±0.3	3.6±0.2	3.6±0.2
PCC	20.1±1.5	16.7±0.6	8.2±0.8	7.6±0.6	0.7±0.2	8.1±0.2	1.8±0.1	3.1±0.1	4.6±0.1

Note: values indicate across subject averages ± standard deviation.

Low resolution dynamic analysis

For the low-resolution dynamic analysis of the visual cortex data, we used a sliding window (width, 128 acquisitions; step size, 2 acquisition) to measure average metabolite concentration as it changed over the course of the run (256 acquisitions/768 sec). For the posterior cingulate cortex data, we matched the duration of the sliding window width to the that used for the visual cortex data by including more acquisitions (width, 192 acquisitions; step size, 2 acquisition), and measured metabolite concentrations as they changed over the course of the run (320 acquisitions/640 sec). Prior to running analyses, metabolite concentration data were screened to remove noisy and/or spurious quantifications. In

particular, we removed individual traces for which the concentration changed by more than 50% (GABA+/Glx) or 5% (tCr/NAA) or the standard deviation was greater than three standard deviations from the average standard deviation. This resulted in omission of data from three subject's data in the visual cortex analyses and 8, 7, and 3 subjects from the posterior cingulate cortex analysis of GABA+, Glx and NAA, respectively. To remove spurious significant differences in the time course, a cluster correction was applied. Clusters were defined by the sum of their constituent (absolute) *t*-values and compared to a null hypothesis distribution of clusters produced by shuffling the time labels (1000 permutations); positive and negative *t*-value clusters were treated sepatarely. Clusters below the 95th percentile of the null hypothesis distribution were disregarded.

High resolution dynamic analysis

The temporal resolution of MRS is severely limited by signal-to-noise ratio of individual spectra. That is, to achieve the signal-to-noise ratio required to yield an accurate metabolic measurement, many individual spectra must be combined. In the low-resolution dynamic analysis, to achieve sufficiently high signal we combined multiple (128) spectra within the same subject. This method produces a dynamic trace for each participant; however, the smoothing produced by the sliding window approach may obscure both the true magnitude of metabolic change over time and dynamic changes occurring at higher frequency. Thus, to achieve higher temporal resolution, we averaged individual 'ON' and 'OFF' spectra across participants to produce a single trace (temporal resolution, 2 acquisitions), with no smoothing, for each condition. Note, due to the necessity of large a sample size, this analysis was only performed with the primary datasets. Prior to running analyses, metabolite concentration data were screened to remove noisy and/or spurious quantifications. Specifically, we removed relative concentration values (GABA+/Glx:tCR) that were above 0.4 before removing values that were more than three standard deviations from the mean. This resulted in omission of six GABA+:tCr data points from the posterior cingulate cortex analysis. To remove spurious significant differences in the cross-correlation analyses, a bootstrapping correction was applied. A null hypothesis coefficient distribution was produced by shuffling the time labels (5000 permutations). We calculated correlation values at ten different lags; to correct for multiple comparisons we used a Bonferroni corrected alpha value to determine the critical coefficient value for each null hypothesis distribution. Thus, coefficient values below the 0.50th percentile of the null hypothesis distribution of cross-correlation analyses were disregarded.

RESULTS

Low resolution temporal dynamics of GABA and Glx

Using a sliding temporal window analysis, we quantified change in the concentration of GABA+ and Glx measured from MRS voxels targeting visual and posterior cingulate cortices over the course of 13 and 12 min periods, respectively. We found that in the visual cortex GABA+ significantly decreased (~4%) while Glx significantly increased (~2%) over the course of the period (**Fig. 2a**). By comparison, we found that in the posterior cingulate cortex there was no significant change in either GABA or Glx (**Fig. 2b**). Given that we referenced GABA+ and Glx to tCr, a possible concern is that the changes in metabolite concentration observed in the visual cortex reflect changes in tCr, as opposed to GABA+ or Glx. However, this is unlikely as we did not find similar changes in NAA, which was also referenced for tCr (**Fig. 2a**).

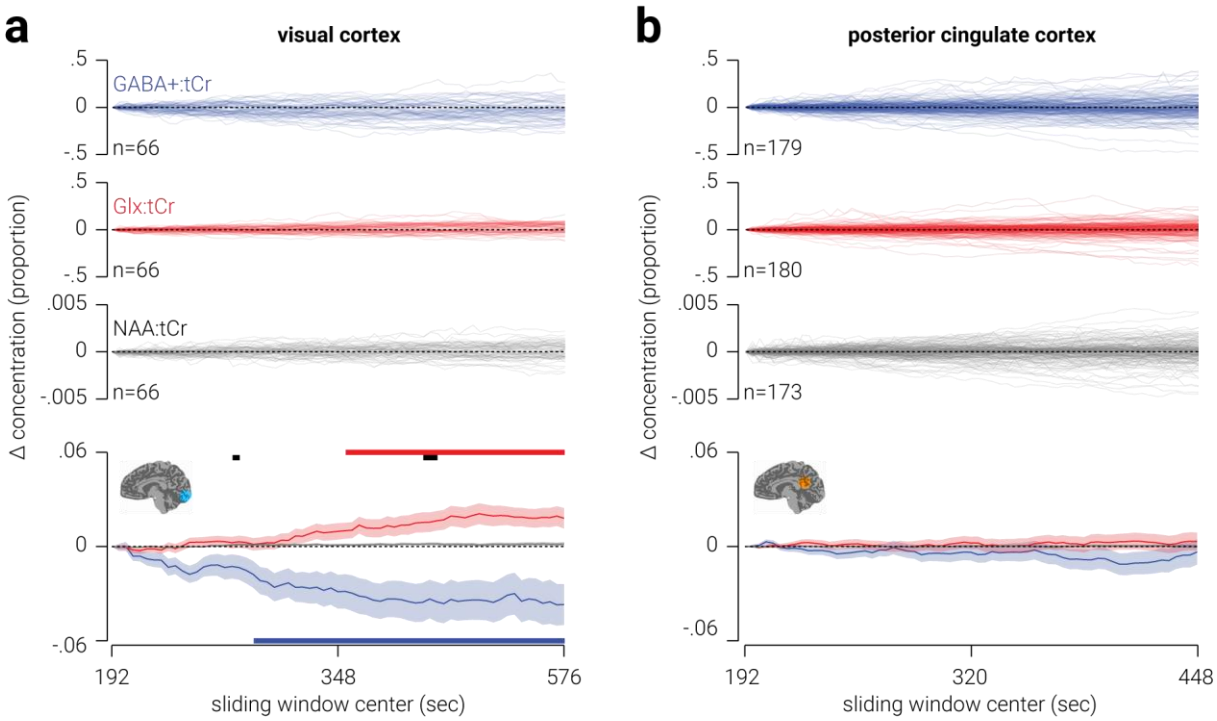

Figure 2. Low resolution temporal dynamics of metabolites in visual and posterior cingulate cortex. (**a**, top) Individual traces showing change in GABA+, Glx, and NAA (all referenced to tCr) measured from a MRS voxel targeting the visual cortex. (**a**, bottom) Same as (**a**, top), but averaged across participants. (**b**) Same as (**a**), but from a MRS voxel targeting the posterior cingulate cortex. Shaded regions indicate s.e.m. and horizontal coloured bars at the top and bottom of (**a**) indicate (cluster corrected) periods of significant difference from zero.

For each voxel location, we assessed whether there were relationships between different static metabolite concentrations or changes in different concentrations. For static measurements, we averaged across all 256/320 acquisitions. The results of the analysis are

shown in Table 2. For static metabolite concentrations, we found a positive relationship between Glx and NAA measured from both visual and posterior cingulate cortex. We also found a positive correlation between GABA+ and NAA in the visual cortex, and between GABA+ and Glx in the posterior cingulate cortex. By contrast, we found no relationships between the change in different metabolite concentrations.

Table 2. Correlation coefficients between metabolites measured from visual and posterior cingulate cortices

Location	GABA+ & Glx	GABA+ & NAA	Glx & NAA	ΔGABA+ & ΔGlx	ΔGABA+ & ΔNAA	ΔGlx & ΔNAA
VC	-0.10	0.38**	0.32**	0.15	-0.14	0.06
PCC	0.25***	0.17	0.49***	0.06	0.07	<.01

Note: Correlation coefficients are partial coefficients after controlling for the common reference metabolite tCr; VC and PCC denote visual and posterior cingulate cortex; all metabolites are referenced to tCr and tissue-corrected; single, double, and triple asterisks indicate P<.05, P<.01, and P<.001, respectively.

Previous MRS work compared static measurements of GABA+ and Glx concentration taken from a voxel targeting the visual cortex while participants either had their eyes closed, open in the darkness, or open while viewing a dynamic checkerboard stimulus (Kurcyus et al., 2018). This work revealed that GABA+ concentrations were higher when participants had their eyes closed, compared to open in darkness, while Glx concentration was lower when participants eyes were closed, compared to when receiving visual stimulation. We did not acquire data from participants under different viewing conditions; however, we found that the concentration of GABA+ and Glx changed over the course of the scan when participants had their eyes closed. As a further test of this result, we reanalysed the data from Kurcyus et al. (2018), henceforth referred to as the K-dataset, using our dynamic sliding analysis.

As a sanity check, we first analysed the K-dataset using the standard static analysis, replicating the pattern of results found in the previous study (**Fig. 3a-b**; Kurcyus et al., 2018). Additionally, we applied this analysis to NAA, for which we found no significant differences between conditions (**Fig. 3c**). We then applied a sliding temporal window analysis to the data to test for dynamic trends in metabolite concentration. We found there was an increase in Glx and NAA in the stimulus condition, however, we found no other significant differences for GABA+, Glx, or NAA across the three conditions (**Fig. 3d-f**). The eyes closed condition of the K-dataset is analogous to our previously presented visual cortex dataset, so we may have expected to find a similar pattern of results, i.e., a decrease in GABA+ and an increase in Glx. However, the scan duration of the K-dataset was only two thirds that of ours. Indeed, in the period captured by the sliding window analysis of the K-dataset, Glx in our dataset had not yet significantly risen above zero and GABA+ had only just begun to reduce significantly below zero (**Fig. 3d**, dotted lines). Further, there is fewer than half the number of scans in the K-

dataset, thus less power to detect a difference. Despite these differences, the numerical pattern of results from the closed eyes condition of the K-dataset is similar to ours: the average change in concentration GABA+ and Glx is always negative and positive, respectively. By contrast, while in the eyes open and stimulus conditions the average change in concentration of Glx is always positive, GABA+ is less consistently negative than in the eyes closed condition.

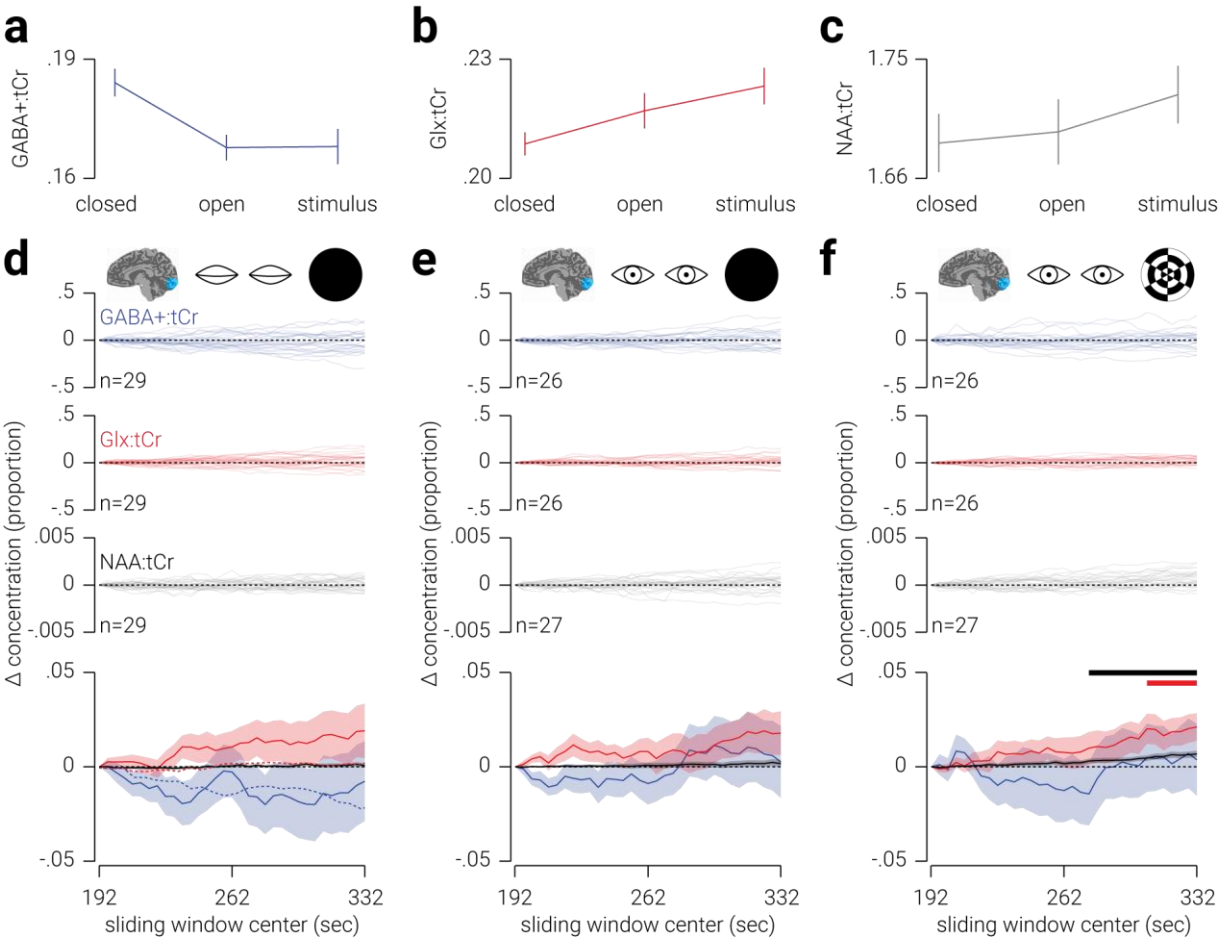

Figure 3. Low resolution temporal dynamics of metabolites in visual cortex during different viewing conditions. Static average concentration of (**a**) GABA+, (**b**) Glx, and (**c**) NAA measured from a MRS voxel targeting the visual cortex when participants have their eyes closed, open in darkness, or open while viewing a dynamic checkerboard stimulus; data is reanalysed from (Kurcyus et al., 2018). (**d**, top) Individual traces showing change in GABA+, Glx, and NAA in the visual cortex when participants have their eyes closed. (**d**, bottom) Same as (**d**, top), but averaged across participants. For comparison, the dotted lines show the results from the visual cortex dataset of the main analysis. (**e** & **f**) Same as (**d**), but while participants have their eyes open in (**e**) darkness or (**f**) while viewing a dynamic checkerboard stimulus. All metabolite concentrations are referenced to tCr and tissue-corrected using a CSF correction. Error bars in (**a**-**c**) and shaded regions in (**d**-**f**) indicate s.e.m. and horizontal coloured bars at the top and bottom of (**f**) indicate (cluster corrected) periods of significant difference from zero.

High resolution temporal dynamics of GABA and Glx

In the previous analysis we used a temporal sliding window to measure change in metabolite concentrations over time. The signal-to-noise of MRS measurements constrains the minimum window size that can be applied with this analysis. To overcome this limitation, we used a novel approach in which measurements are combined across subjects to achieve the maximum temporal resolution afforded by the relaxation time of the acquisition, e.g., 3 sec. In the visual cortex, we found change in GABA+, relative from the first measurement, was primarily negative, with a minimum of -25%, while change in Glx was primarily positive, with maximum of 16% (**Fig. 4a**). These results are consistent with those from the previous analysis, except the higher temporal resolution obtained with the current approach revealed considerably larger changes in metabolite concentration than the previous estimates, which were likely obscured by smoothing measurements across the temporal window. In the posterior cingulate cortex, we found that change in both GABA+ and Glx was primarily negative, and similar in amplitude (**Fig. 4b**).

While GABA and Glx are thought to support opposing mechanisms in the central nervous system, i.e., inhibition and excitation, it seems reasonable to expect interactions between these metabolites. For example, Gln is a primary source of GABA synthesis (Patel, Rothman, Cline, & Behar, 2001; Paulsen, Odden, & Fonnum, 1988; Rae et al., 2003). Indeed, we found that the static concentration of GABA+ and Glx were positively related in the posterior cingulate cortex. However, we found no evidence for a relationship between the overall changes in these metabolites in either the visual or posterior cingulate cortex (Table 2). One reason for this may be that the relationship between these metabolites may only be observed at a temporally high resolution, but not averaged across a 12/13 minute period. To test this hypothesis, we used the high temporal resolution metabolite measurements to perform cross-correlation analyses on GABA+ and Glx concentration.

For the visual cortex, we found that the concentration of GABA+ significantly predicted the concentration of Glx both 18 (time points=125, Pearson r=-.27, P=.003) and 30 (time points=123, Pearson r=-.31, P=5.0e^{-4}; **Fig. 4c**, top) sec later. In particular, an increase in GABA+ predicted a decrease Glx both 18 and 30 sec later. By contrast, Glx was not found to predict GABA+ at any lag within a range of 60 sec. For the posterior cingulate cortex, we found a strikingly similar pattern of results: GABA+ significantly predicted Glx (lag=32 sec, time points=143, Pearson r=-.21, P=.013; **Fig. 4c**, bottom) at the lag nearest that found for the same relationship in the visual cortex (30 sec). Further, the direction of prediction was the same in both visual and posterior cingulate cortices, that is, an increase in GABA+ predicted a subsequent decrease Glx.

A possible concern is that the relationship between GABA+ and Glx was the influenced by their common reference metabolite (tCr). However, we found that GABA+ also predicts Glx

30 sec later in both cortical areas when NAA, rather than tCr, is used as a reference metabolite (visual cortex: lag = 30 s, time points=123, Pearson *r*=-.33, *P*=2.0e^{-4}; posterior cingulate cortex: lag = 32 s, time points=143, Pearson *r*=-.25, *P*=.002; **Fig. 4d**). Another possible concern with this new analysis is that the signal-to-noise ratio is insufficiently high to yield valid measurements, e.g., due to poor peak fitting. To assess the validity of the measurements, we attempted to reproduce the results from the low-resolution temporal analysis by applying a sliding window to the high-resolution metabolite trace. If the high-resolution measurements are valid, we should see a correspondence between the average results from the low-resolution analysis and those produced by applying a sliding temporal window to the high-resolution measurements. For the visual cortex, we found a very high correlation between the measurements produced by the two analyses for both GABA+ (n=65, r=.988, P<1.0e^{-10}; **Fig. 4e**, top) and Glx (n=65, r=.998, P<1.0e^{-10}). For the posterior cingulate cortex, we also found a significant correspondence between the two measurements (GABA+: n=65, r=.720, P<1.0e^{-10}; **Fig. 4e**, bottom) and Glx (n=65, r=.501, P=1.6e^{-5}). These results support the validity of the high-resolution measurements and the results of the cross-correlation analysis.

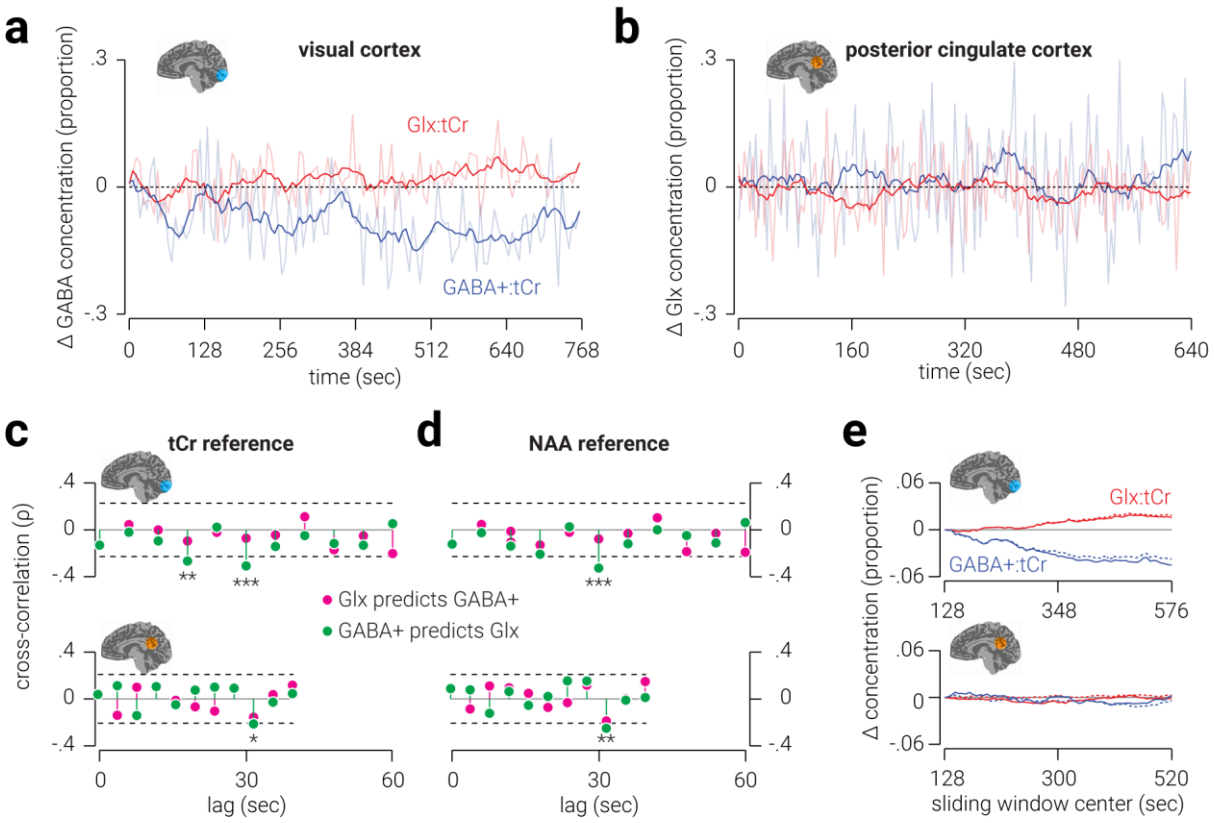

Figure 4. High resolution temporal dynamics of metabolites in visual and posterior cingulate cortex. Change in GABA+ and Glx concentration, referenced to tCr and averaged across subjects, measured from voxels targeting **a**) visual and **b**) posterior cingulate cortices. Semi-transparent lines indicate raw measurement values and opaque lines indicate smoothed values (window size, 8 measurements). (**c**) Cross-correlations between GABA+ and Glx, referenced to tCr, measured from voxels targeting (top) visual and (bottom) posterior cingulate cortices. The horizontal black dashed lines indicate the Bonferroni corrected null hypothesis coefficient thresholds established by the permutation described in the Methods. Single-, double, and triple- asterisks indicate $P<.05$, $P<.01$, $P<.001$, respectively. (**d**) Same as (**c**), but referenced to NAA. Comparison between results from sliding window method used in the low temporal resolution analysis (dashed lines) and sliding window applied to results from high resolution analysis (solid lines) for (**e**, top) visual and (**e**, bottom) posterior cingulate cortices.

DISCUSSION

MRS can be used in vivo to differentiate types of neural activity, e.g., inhibitory and excitatory, and provide evidence for the involvement of different neurotransmitter systems in cognitive processes. In MRS studies, temporal resolution is typically sacrificed to achieve sufficient signal-to-noise ratio to produce a reliable estimate of metabolite concentration. Here we use novel analyses with large datasets to reveal the dynamics of GABA+ and Glx in visual and posterior cingulate cortices. We replicate previously established relationships between metabolites measured using the standard approach. We use a sliding window approach to show that the dynamic concentrations of GABA+ and Glx in the visual cortex drifts in opposite directions, that is, GABA+ decreases while Glx increases over time. We then use a new method of combining MRS measurements across subjects, as opposed to time, to produce a high temporal resolution index of metabolite concentration. Using this approach, we find that in both the visual and posterior cingulate cortices, the concentration of GABA+ predicts that of Glx ~30 sec later, such that an increase in GABA+ is correlated with a subsequent reduction in Glx.

Dynamic response of GABA and Glx in the visual cortex

Several studies have investigated GABA and/or Glx/Glu concentration in the visual cortex in response to different viewing conditions. Mekle et al. (2017) found a ~5% reduction in GABA concentration in response to visual stimulation. By contrast, while Kurcyus et al. (2018) reported that GABA was 16% lower when participants had their eyes open with no visual stimulation compared to when closed, they, like others (Bednařík et al., 2015; Mangia et al., 2007; Schaller, Mekle, Xin, Kunz, & Gruetter, 2013), found no evidence for a difference in GABA in response to visual stimulation. Based on these somewhat inconsistent findings, one may infer that visual stimulation, or merely having the eyes open, leads to a reduction in the concentration of GABA in the visual cortex. Extending this rationale, one could predict that closing the eyes should produce an increase in GABA. By contrast, we found the opposite result: during a 13 min period of resting, in which participants' eyes were closed, the concentration of GABA+ in the visual cortex reduced on average by ~4%.

Our reanalysis of data comparing metabolite concentration in the visual cortex under different viewing conditions suggests that these results may not be mutually exclusive. Consistent with the original study, we found that static measurements of GABA+ indicated concentrations were higher when participants had their eyes closed. Despite this, dynamic analysis of the data indicated a trend towards reduction in concentration over time. This pattern of results was more consistent when participants had their eyes closed than when open in the darkness or during visual stimulation. Indeed, our results are consistent with

previous work showing that monocular deprivation leads to reduced GABA concentration (~8%) in the visual cortex, but not the posterior cingulate cortex, relative a pre-deprivation baseline measurement (Lunghi, Emir, Morrone, & Bridge, 2015). Thus, our finding that GABA is reduced when both eyes are closed may indicate that visual deprivation, either monocular or binocular, produces a reduction in the concentration of GABA in the visual cortex.

Previous observations of Glx concentration in the visual cortex have been more consistent; several studies have shown Glx/Glu concentration increases (2-4%) in response to visual stimulation (Bednařík et al., 2015; Hall, Barnes, Furlong, Seri, & Hillebrand, 2010; Kurcyus et al., 2018; Lin, Stephenson, Xin, Napolitano, & Morris, 2012; Mangia et al., 2007; Schaller et al., 2013). Similar to our results for GABA, our observation that Glx increases with the eyes closed appears to defy previous findings. However, as previously noted, while our results may be surprising, they are not mutually exclusive with the findings of previous studies. Clearly, more work is needed it disambiguate changes in metabolite concentration that occur in the visual cortex at different time scales.

To produce a high temporal resolution measure of metabolite concentrations, we applied a novel approach in which we combined MRS acquisitions across subjects, rather than time. This approach yields a single measurement of metabolite concentration as a function of time; thus, we cannot test the statistical significance of the changes observed over time. However, it is reasonable to assume that the changes observed using the sliding temporal window or static approaches underestimate the true magnitude of change, due to averaging. Measurements produced by combining acquisitions across subjects provide an indication of the true magnitude of change in GABA+ and Glx during the scan: up to ~20% for GABA+ and ~5% for Glx.

Dynamic relationship between GABA and Glx

A common factor of studies of GABA and Glx/Glu in the visual cortex is that these metabolites consistently change in opposite directions, and not in the same direction (Kurcyus et al., 2018; Mekle et al., 2017; Rideaux et al., 2019). This pattern would suggest an interdependency between the two metabolites. Given that Gln is a primary source of GABA synthesis (Patel et al., 2001; Paulsen et al., 1988; Rae et al., 2003), one may expect that a change in the concentration of GABA may result in a corresponding change in Glx (Gln and Glu), or vice versa. In line with this, our high temporal resolution analysis of the data revealed a striking cross-correlation between these metabolites which was evident in both the visual and posterior cingulate cortices. Specifically, we found that the concentration of GABA+ predicts the concentration of Glx ~30 sec later. This relationship is obscured by conventional approaches of MRS analysis; indeed, we found no evidence for a relationship between the overall change in GABA+ and Glx in either location.

A limitation of MRS is that it measures the total concentration of neurochemicals within a localized region and cannot distinguish between intracellular and extracellular pools of GABA. It is generally thought that intracellular vesicular GABA drives neurotransmission (Belelli et al., 2009), whereas extracellular GABA maintains tonic cortical inhibition (Martin & Rimvall, 1993). Synthesis of intracellular GABA from Gln via the GABA-Gln cycle occurs on the scale of milliseconds, so it seems unlikely that this metabolic association could explain the predictive relationship between GABA and Glx concentration 30 sec later. Instead, this relationship may reflect changes in the level of extracellular GABA, followed by relatively sluggish changes in the concentration of Glu to maintain the balance of inhibition and excitation.

Conclusion

The relatively low signal-to-noise of MRS measurements has shaped the types of questions that the technique has been used to address. Here we overcome this limitation by combining data from large cohorts to examine the dynamics of GABA and Glx concentration in the visual cortex. Through use of existing and novel analyses, we reveal opposing dynamic shifts in GABA and Glx in the visual cortex while participants are at rest. Further, we demonstrate a predictive relationship between GABA and Glx that is present in both visual and posterior cingulate cortices. This study exposes temporal trends of primary neurotransmitters in the visual cortex, but more generally, these findings demonstrate the feasibility of using MRS to investigate in vivo dynamic changes of metabolites.

Acknowledgements

The work was supported by the Leverhulme Trust (ECF-2017-573), the Issac Newton Trust (17.08(o)), and the Wellcome Trust (095183/Z/10/Z). I acknowledge the assistance of Katarzyna Kurcyus, Valentin Riedl, Mark Mikkelsen, and Richard Edden in supplying their data for reanalysis.

REFERENCES

Bednařík, P., Tkáč, I., Giove, F., Dinuzzo, M., Deelchand, D. K., Emir, U. E., … Mangia, S. (2015). Neurochemical and BOLD responses during neuronal activation measured in the human visual cortex at 7 Tesla. *Journal of Cerebral Blood Flow and Metabolism*, *35*(10), 601–610. https://doi.org/10.1038/jcbfm.2014.233

Belelli, D., Harrison, N. L., Maguire, J., Macdonald, R. L., Walker, M. C., & Cope, D. W. (2009). Extrasynaptic GABAA Receptors: Form, Pharmacology, and Function. *Journal of Neuroscience*, *29*(41), 12757–12763. https://doi.org/10.1523/JNEUROSCI.3340-09.2009

Edden, R. A. E., Muthukumaraswamy, S. D., Freeman, T. C. A., & Singh, K. D. (2009). Orientation Discrimination Performance Is Predicted by GABA Concentration and Gamma Oscillation Frequency in Human Primary Visual Cortex. *Journal of Neuroscience*, *29*(50), 15721–15726. https://doi.org/10.1523/JNEUROSCI.4426-09.2009

Edden, R. A. E., Puts, N. A. J., Harris, A. D., Barker, P. B., & Evans, C. J. (2014). Gannet: A batch-processing tool for the quantitative analysis of gamma-aminobutyric acid-edited MR spectroscopy spectra. *Journal of Magnetic Resonance Imaging*, *40*(6), 1445–1452. https://doi.org/10.1002/jmri.24478

Hall, S. D., Barnes, G. R., Furlong, P. L., Seri, S., & Hillebrand, A. (2010). Neuronal network pharmacodynamics of GABAergic modulation in the human cortex determined using pharmaco-magnetoencephalography. *Human Brain Mapping*, *31*(4), 581–594. https://doi.org/10.1002/hbm.20889

Ip, I. B., Berrington, A., Hess, A. T., Parker, A. J., Emir, U. E., & Bridge, H. (2017). Combined fMRI-MRS acquires simultaneous glutamate and BOLD-fMRI signals in the human brain. *NeuroImage*, *155*, 113–119. https://doi.org/10.1016/J.NEUROIMAGE.2017.04.030

Jansen, J. F. A., Backes, W. H., Nicolay, K., & Kooi, M. E. (2006). ^{1}H MR Spectroscopy of the Brain: Absolute Quantification of Metabolites. *Radiology*, *240*(2), 318–332. https://doi.org/10.1148/radiol.2402050314

Kreis, R., Ernst, T., & Ross, B. D. (1993). Development of the human brain: In vivo quantification of metabolite and water content with proton magnetic resonance spectroscopy. *Magnetic Resonance in Medicine*, *30*(4), 424–437. https://doi.org/10.1002/mrm.1910300405

Kurcyus, K., Annac, E., Hanning, N. M., Harris, A. D., Oeltzschner, G., Edden, R. A. E., & Riedl, V. (2018). Opposite Dynamics of GABA and Glutamate Levels in the Occipital Cortex during Visual Processing. *The Journal of Neuroscience*, *38*(46), 9967–9976. https://doi.org/10.1523/JNEUROSCI.1214-18.2018

Lin, Y., Stephenson, M. C., Xin, L., Napolitano, A., & Morris, P. G. (2012). Investigating the metabolic changes due to visual stimulation using functional proton magnetic resonance spectroscopy at 7 T. *Journal of Cerebral Blood Flow and Metabolism*, *32*(8), 1484–1495.

https://doi.org/10.1038/jcbfm.2012.33

Lunghi, C., Emir, U. E., Morrone, M. C., & Bridge, H. (2015). Short-Term monocular deprivation alters GABA in the adult human visual cortex. *Current Biology*, *25*(11), 1496–1501. https://doi.org/10.1016/j.cub.2015.04.021

Mangia, S., Tkáč, I., Gruetter, R., Van de Moortele, P.-F., Maraviglia, B., & Uğurbil, K. (2007). Sustained Neuronal Activation Raises Oxidative Metabolism to a New Steady-State Level: Evidence from ^{1}H NMR Spectroscopy in the Human Visual Cortex. *Journal of Cerebral Blood Flow & Metabolism*, *27*(5), 1055–1063. https://doi.org/10.1038/sj.jcbfm.9600401

Martin, D. L., & Rimvall, K. (1993, February). Regulation of γ- Aminobutyric Acid Synthesis in the Brain. *Journal of Neurochemistry*. Blackwell Publishing Ltd. https://doi.org/10.1111/j.1471-4159.1993.tb03165.x

Mekle, R., Kühn, S., Pfeiffer, H., Aydin, S., Schubert, F., & Ittermann, B. (2017). Detection of metabolite changes in response to a varying visual stimulation paradigm using short-TE 1H MRS at 7 T. *NMR in Biomedicine*, *30*(2), e3672. https://doi.org/10.1002/nbm.3672

Mikkelsen, M., Barker, P. B., Bhattacharyya, P. K., Brix, M. K., Buur, P. F., Cecil, K. M., … Edden, R. A. E. (2017). Big GABA: Edited MR spectroscopy at 24 research sites. *NeuroImage*, *159*, 32–45. https://doi.org/10.1016/j.neuroimage.2017.07.021

Mikkelsen, M., Harris, A. D., Edden, R. A. E., & Puts, N. A. J. (2018). Macromolecule-suppressed GABA measurements correlate more strongly with behavior than macromolecule-contaminated GABA+ measurements. *Brain Research*, *1701*, 204–211. https://doi.org/10.1016/J.BRAINRES.2018.09.021

Mikkelsen, M., Rimbault, D. L., Barker, P. B., Bhattacharyya, P. K., Brix, M. K., Buur, P. F., … Edden, R. A. E. (2019). Big GABA II: Water-referenced edited MR spectroscopy at 25 research sites. *NeuroImage*, *191*, 537–548. https://doi.org/10.1016/J.NEUROIMAGE.2019.02.059

Mullins, P. G., McGonigle, D. J., O'Gorman, R. L., Puts, N. A. J., Vidyasagar, R., Evans, C. J., … Wilson, M. (2014). Current practice in the use of MEGA-PRESS spectroscopy for the detection of GABA. *NeuroImage*, *86*, 43–52. https://doi.org/10.1016/j.neuroimage.2012.12.004

Patel, A. B., Rothman, D. L., Cline, G. W., & Behar, K. L. (2001). Glutamine is the major precursor for GABA synthesis in rat neocortex in vivo following acute GABA-transaminase inhibition. *Brain Research*, *919*(2), 207–220. https://doi.org/10.1016/S0006-8993(01)03015-3

Paulsen, R. E., Odden, E., & Fonnum, F. (1988). Importance of glutamine for gamma-aminobutyric acid synthesis in rat neostriatum in vivo. *Journal of Neurochemistry*, *51*(4), 1294–1299. https://doi.org/10.1111/j.1471-4159.1988.tb03099.x

Rae, C., Hare, N., Bubb, W. A., McEwan, S. R., Bröer, A., McQuillan, J. A., … Bröer, S. (2003). Inhibition of glutamine transport depletes glutamate and GABA neurotransmitter pools: Further evidence for metabolic compartmentation. *Journal of Neurochemistry*, *85*(2), 503–514. https://doi.org/10.1046/j.1471-4159.2003.01713.x

Rideaux, R., Goncalves, N. R., & Welchman, A. E. (2019). Mixed-polarity random-dot stereograms alter GABA and Glx concentration in the early visual cortex. *Journal of Neurophysiology*, *122*(2), 888–896. https://doi.org/10.1152/jn.00208.2019

Rowland, L. M., Pradhan, S., Korenic, S. A., Wijtenburg, S. A., Hong, L. E., Edden, R. A. E., & Barker, P. B. (2016). Elevated brain lactate in schizophrenia: a 7 T magnetic resonance spectroscopy study. *Translational Psychiatry*, *6*(11), e967. https://doi.org/10.1038/tp.2016.239

Schaller, B., Mekle, R., Xin, L., Kunz, N., & Gruetter, R. (2013). Net increase of lactate and glutamate concentration in activated human visual cortex detected with magnetic resonance spectroscopy at 7 tesla. *Journal of Neuroscience Research*, *91*(8), 1076–1083. https://doi.org/10.1002/jnr.23194